Journal of Catalysis **211,** 165–172 (2002)
doi:10.1006/jcat.2002.3726

# *n*-Butene Conversion on H-Ferrierite Studied by $^{13}C$ MAS NMR

Alexander G. Stepanov,*[,1] Mikhail V. Luzgin,* Sergei S. Arzumanov,* Horst Ernst,† and Dieter Freude†[,2]

*Boreskov Institute of Catalysis, Siberian Branch, Russian Academy of Sciences, Prospekt Akademika Lavrentieva 5, Novosibirsk 630090, Russia; and †Abteilung Grenzflächenphysik, Universität Leipzig, Linnéstraße 5, 04103 Leipzig, Germany

Received March 5, 2002; revised June 6, 2002; accepted June 19, 2002

**$^{13}C$ MAS NMR analysis of the hydrocarbon products formed from the selectively $^{13}C$-labeled *n*-but-1-ene on zeolite ferrierite (H-FER) in a closed batch reactor revealed the following successive steps of the olefin conversion with temperature increase from 300 to 823 K: a double-bond-shift reaction, scrambling of the selective $^{13}C$ label in the formed *n*-but-2-ene, oligomerization (dimerization), conjunct polymerization, formation of condensed aromatics, and formation of the simple aromatics. Arguments in favor of either bimolecular or pseudo-monomolecular mechanisms are provided, excluding at the same time the monomolecular isomerization of *n*- to isobutene on a fresh sample. The arguments are based on selective label redistribution in the *n*-but-2-enes, the impossibility of the existence of isobutene inside the pores of the zeolite under static conditions and the observation of *n*-but-2-enes oligomerization (dimerization). Conjunct polymerization leads to the formation of alkyl-substituted cyclopentenyl cations (CPCs), which can serve as an intermediate for pseudo-monomolecular isomerization. Carbonaceous deposits (polycyclic aromatics), which deactivate the catalyst in the isomerization reaction, are formed from the CPCs. Polycyclic aromatics are transformed into simple aromatics with methane and ethane evolution at 823 K.** 

*Key Words:* ***n*-butene; H-FER zeolite; isomerization; conjunct polymerization; $^{13}C$-label scrambling; reaction mechanism; $^{13}C$ MAS NMR spectroscopy.**

## 1. INTRODUCTION

Zeolite H-FER, the hydrogen form of ferrierite (1), represents a high-efficiency catalyst for isomerization of *n*-butene into isobutene (2, 3). Industrial demands for isobutene are due to its use in the synthesis of methyl *tert*-butyl ether (MTBE), an important component of the gasoline pool. High selectivity and stability of the ferrierite in the isomerization of *n*- to isobutene (2, 3) stimulated numerous studies of the mechanism of this reaction (3–17). Monomolecular, bimolecular, and pseudo-monomolecular mechanisms have been claimed for this reaction by studying the products distribution (3), the changes of the selectivity in the products with time on stream (5, 6, 9) and the $^{13}C$ isotopic label redistribution (6, 12) from the reagent into the reaction products.

A bimolecular reaction pathway with simultaneous formation of a large quantity of $C_3$ and $C_5$ olefins was first suggested by Mooiweer *et al*. (3). Meriaudeau *et al*. (6) proposed that a bimolecular mechanism operates on the fresh and nonselective ferrierite catalyst, whereas a monomolecular reaction takes place for the coked and selective catalyst. The conclusion about a bimolecular mechanism at the outer surface of the catalyst was made based on the poor selectivity for isobutene formation and observation of the double $^{13}C$-labeled isobutene from the single $^{13}C$-labeled *n*-butene in the reaction products (6–8). The increased selectivity of isobutene formation in parallel with the decreased total activity of the coked catalysts and the yield of the single $^{13}C$-labeled isobutene from the single labeled *n*-butene were the main arguments in favor of a monomolecular isomerization mechanism inside the zeolite channels (4, 6, 8). The monomolecular mechanism includes the formation of a high-energy primary carbenium ion (18, 19). A pseudo-monomolecular mechanism was assumed by Guisnet *et al.* (9–11). It excludes the formation of a primary cation and involves the participation of the coke deposits generating intermediate benzylic cations as the active sites near the outer surface of the crystallites. But the formation of benzylic cations was so far not experimentally proved and other cationic species may be involved in the reaction.

Various spectroscopic techniques were used to characterize the adsorbed species and clarify the reaction mechanism (6–16, 20, 21). UV-vis and FTIR spectroscopic studies characterized the adsorbed species, precursors of isobutene and high-temperature coke deposits (11–13, 15, 16, 20, 21), whereas $^{13}C$ NMR and GC-MS monitored the $^{13}C$ label redistribution from *n*-butene to isobutene showing the difference in the reaction mechanisms on fresh and coked catalysts (6, 12).

$^{13}C$ MAS NMR spectroscopy is a well-established technique for the study of the mechanisms of heterogeneous

[1] To whom correspondence should be addressed. Fax: +49 341 97 32549. E-mail: freude@physik.uni-leipzig.de.

[2] To whom correspondence should be addressed. Fax: +7 (3832) 34 30 56. E-mail: a.g.stepanov@catalysis.nsk.su.



0021-9517/02 $35.00

catalysis (22–30). The redistribution of the selective $^{13}C$ label from the initial reactants in the reaction products in the course of the reaction identifies the adsorbed reaction products and allows conclusions about the reaction mechanism. In a recent study, Philippou *et al.* (17) observed the formation of butene dimers and explained it through the bimolecular mechanism.

This paper explains the successive steps of conversion of *n*- to isobutene under static conditions. We provide evidence against a monomolecular isomerization and support a bimolecular mechanism of isomerization on fresh samples. The step of conjunct polymerization was identified, providing the formation of cyclopentenyl cations (CPCs), which can serve as the intermediate for pseudomonomolecular isomerization on the coked sample.

## 2. EXPERIMENTAL

### 2.1. Preparation of the Sample

The zeolite ferrierite (H-FER, Si/Al = 50) was prepared by Prof. Dr. W. Schwieger following the procedure described in the literature (14). The samples were calcined at 673 K for 2 h in air and for 2 h under vacuum ($10^{-3}$ Pa). Then *n*-but-1-ene (about 300 $\mu$mol per gram H-FER) was adsorbed under vacuum by cooling the sample with liquid nitrogen. This loading corresponds to about one molecule per bridging hydroxyl group (≡Si–OH–Al≡) in the ferrierite framework. Labeled [1-$^{13}C$]-*n*-but-1-ene, with the $^{13}C$ isotope (99% $^{13}C$ isotope enrichment) at the terminal olefinic $=CH_2$ group was used. After sealing the glass tube, the samples were kept at the temperature of liquid nitrogen. Before measurements, the samples were warmed to room temperature (~300 K) or heated in an oven for 1 h at 373–823 K. It was shown by additional experiments that the loading of 300 $\mu$mol per gram H-FER could also be achieved under a butene pressure of 5 kPa at 473 K under equilibrium conditions.

### 2.2. NMR Analysis

The reaction products were analyzed in the sealed glass tubes. $^{13}C$ MAS NMR spectra with high-power proton decoupling were recorded at 100.613 MHz on a Bruker MSL-400 spectrometer at room temperature. $^{13}C$ CP/MAS NMR experiments were performed by cross-polarization with a high-power proton decoupling field corresponding to a 5.0-$\mu$s pulse length for the $\pi/2$ pulse, a contact time of 5 ms and a recycle delay of 3 s. One-pulse excitation $^{13}C$ MAS NMR spectra with high-power proton decoupling were recorded using 45° flip angle pulses of 2.5-$\mu$s duration and 10–15-s recycle delay. The spinning rates were 2.7–4.5 kHz. A few thousand scans were collected for each spectrum. Chemical shifts were adjusted to TMS with an accuracy ±0.5 ppm, whereas the precision of the relative line position was 0.1–0.15 ppm.

## 3. RESULTS

### 3.1. Conversion of n-But-1-ene at 300–373 K

*n*-But-1-ene readily undergoes a double-bond-shift reaction when it is adsorbed on H-FER (12, 13, 16, 20). Therefore, one could expect that the signals from the *n*-but-2-enes would be observed in the $^{13}C$ NMR spectrum immediately after the adsorption of [1-$^{13}C$]-*n*-but-1-ene (**1**) on the zeolite. Indeed, the expected signal for the $^{13}C$-labeled $=CH_2$ group at 113 ppm (see Table 1) is not observed for the adsorbed butene **1**. Instead, signals at 17 and 13 ppm appear in the spectrum (see Fig. 1, spectrum b). They arise from the methyl groups of *trans*- and *cis*-*n*-but-2-ene (**2**), respectively. The $^{13}C$-labeled $=CH_2$ group of **1** is transformed into the $^{13}C$-labeled $CH_3$ groups of **2**. The intense signal at 113 ppm due to the $^{13}C$-labeled $=CH_2$ group of **1** is observed in the corresponding spectrum of the Na form of the zeolite, where no transformation of *n*-but-1-ene occurs at 300 K (Fig. 1, spectrum a). This confirms the earlier findings (12, 13, 16, 20) that *n*-but-1-ene undergoes a double-bond-shift reaction yielding a mixture of *trans*- and *cis*-*n*-but-2-enes at low temperatures in zeolite H-FER.

The signal due to the =CH– groups of butenes **2** at 126 ppm appears after keeping the loaded H-FER sample for one week at 300 K. In addition there arise two weak and broad signals at 25 and 33 ppm from butene dimers and oligomers (25, 31, 32) (see Fig. 1, spectrum c). These signals increase if the sample is kept for 1 h at 373 K (see Fig. 1, spectrum d). The signal at 126 ppm indicates that the scrambling of the selective $^{13}C$ label from the methyl groups of butenes **2** into their =CH– groups occurs after a prolonged reaction time even at the low temperature of 300 K. The oligomerization of **2** also proceeds at 300 K. But isobutene signals are not detected. This indicates that there is no isomerization reaction under the static conditions of a batch reactor at room temperature.

**TABLE 1**

**$^{13}C$ NMR Characteristics of *n*-But-1-ene, *trans*- and *cis*-*n*-But-2-enes and Isobutene in Solution[a] and Adsorbed on the Zeolite H-FER**

| Olefin | Chemical shift, $\delta$ (ppm) in solution/adsorbed | | | |
|---|---|---|---|---|
| | $=CH_2$ | =CH–(=C<) | $–CH_2–$ | $CH_3–$ |
| *n*-But-1-ene | 113.2/113 | 140.1/142 | 27.0/28 | 13.4/13 |
| *trans*-*n*-But-2-ene | | 125.42/126 | | 16.4/17 |
| *cis*-*n*-But-2-ene | | 124.22/126 | | 11.42/13 |
| Isobutene[b] | 110.5/111 | 141.4/143 | | 23.7/24 |

[a] Taken from Ref. (34).
[b] Chemical shifts for isobutene on Na-form zeolite is given.

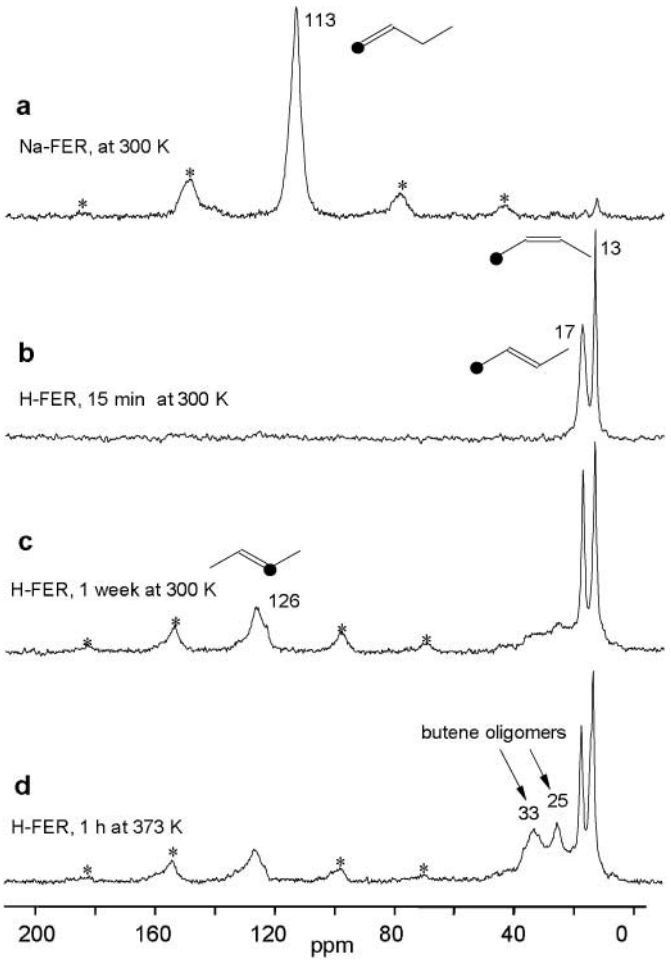


**FIG. 1.** $^{13}$C CP/MAS NMR spectra of the zeolites Na-FER and H-FER loaded with [1-$^{13}$C]-*n*-but-1-ene **1**: (a) Na form kept at 300 K; (b) H form kept for 15 min at 300 K; (c) H form kept for one week at 300 K; (d) H form kept for 1 h at 373 K and then measured at 300 K. Asterisks denote spinning sidebands.

### 3.2. *Conversion of n-But-2-ene and Butene Oligomers at 473–623 K*

Increase of the reaction temperature up to 473 K causes a complete disappearance of the signals from *n*-but-2-enes at 17 and 126 ppm (Fig. 2, spectrum a). The remaining signals at 13, 25, and 33 ppm are due to butene oligomers (dimers) (25, 31, 32). Further increase of the temperature up to 523 K provides alkyl-substituted CPCs with characteristic signals at 152 and 252 ppm (33) and condensed aromatics with signals at 130 and 144 ppm (34) (see Fig. 2, spectrum b). Based on the expected composition of the coke compounds extracted from the zeolite (11), we assign the signal at 130 ppm to methyl-substituted naphthalenic and/or anthracenic compounds, whereas the signal at 144 ppm should be due to fluorenic and/or biphenylic compounds (34). The signals from the butene oligomers at 13, 25, and 33 ppm are still detected after reaction at 473 K. The signals from the paraffins isobutane and isopentane could be identified in the 523 K spectrum, which was obtained without cross-polarization and shows narrow signals due to mobile species (Fig. 3, spectrum a).

After 1-h reaction at 623 K, the signals from the CPC and fluorenic compounds disappear and the signals from naphthalenes remain (Fig. 2, spectrum c). The formation of a mixture of $C_1$–$C_5$ alkanes can be observed at this temperature in Fig. 3 (spectrum b). Butene oligomers were not completely transformed into alkanes and aromatics. The signal at 13 ppm in Figs. 2 (spectrum c) and 3 (spectrum b) proves the existence of a small quantity of oligomers at this temperature.

### 3.3. *Conversion of the Condensed Aromatics and Alkanes Formed from n-But-1-ene at 723–823 K*

Further increase of the reaction temperature causes a complete disappearance of the signal of butene oligomers at 13 ppm. The signals of condensed aromatics, like

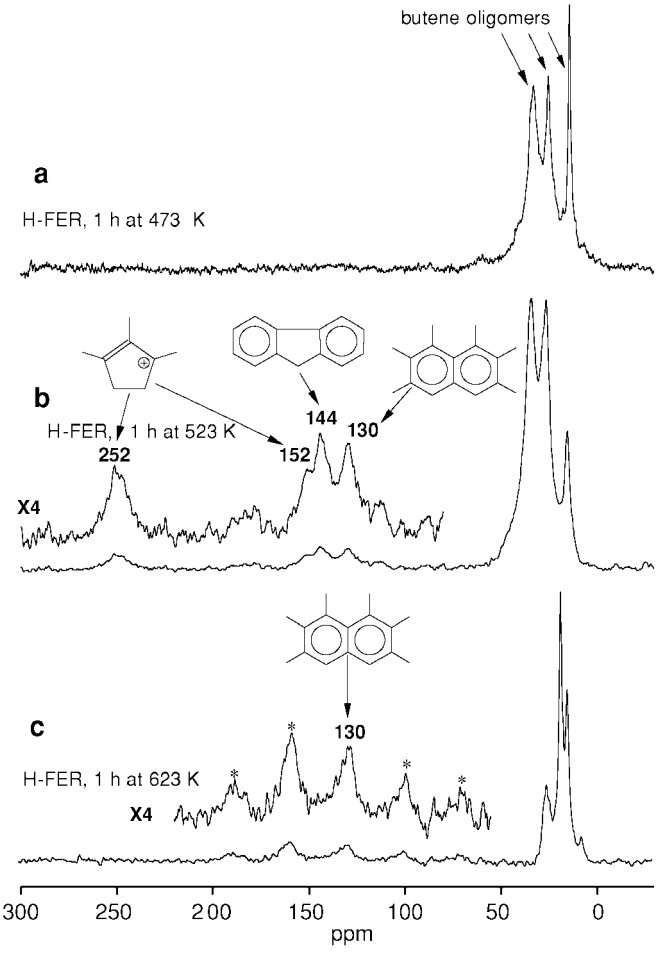


**FIG. 2.** $^{13}$C CP/MAS NMR spectra of [1-$^{13}$C]-*n*-but-1-ene on H-FER zeolite after successive heating of the zeolite sample for 1 h at (a) 473 K, (b) 523 K, and (c) 623 K. Asterisks denote spinning sidebands.

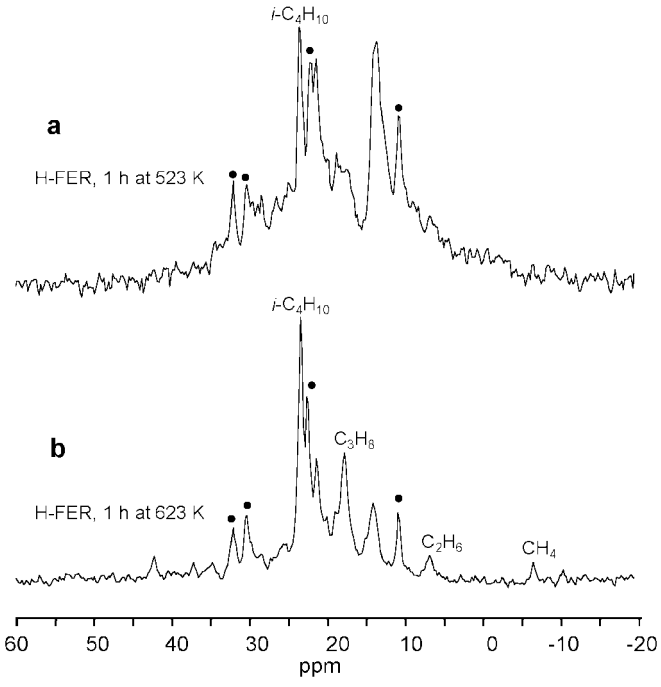


**FIG. 3.** $^{13}C$ MAS NMR spectra of [1-$^{13}C$]-*n*-but-1-ene on H-FER zeolite after reaction at (a) 523 K and (b) 623 K in the region from −20 to +60 ppm. Black dots denote signals from isopentane.

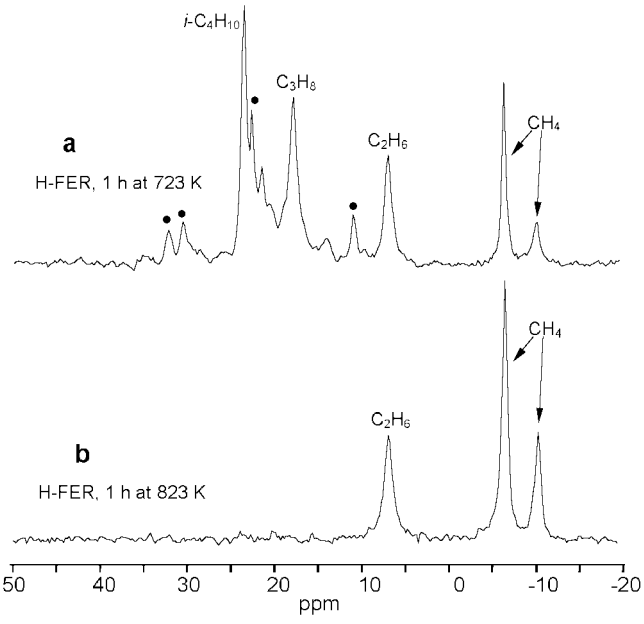


**FIG. 5.** $^{13}C$ MAS NMR spectra of [1-$^{13}C$]-*n*-but-1-ene on H-FER zeolite after reaction at (a) 723 K and (b) 823 K in the region from −20 to +50 ppm. Black dots denote signals from isopentane.

anthracenic compounds with a line at 130 ppm, and $C_1$–$C_5$ alkanes, remain in the spectra after the reaction at 723 K (Figs. 4, spectrum a and 5, spectrum a). At 823 K the condensed aromatics convert to the methyl-substituted simple aromatics and benzene, exhibiting the signal centered at 128 ppm (26, 34). The absence of the signals at 20–22 ppm from the methyl groups of xylenes or toluene (34) supports the conclusion that a notable amount of benzene is formed. The signals from $C_3$–$C_5$ alkanes disappear at this temperature. Only the signals from methane and ethane are observed in the paraffinic spectral region between −20 and +40 ppm (Figs. 4, spectrum b, and 5, spectrum b).

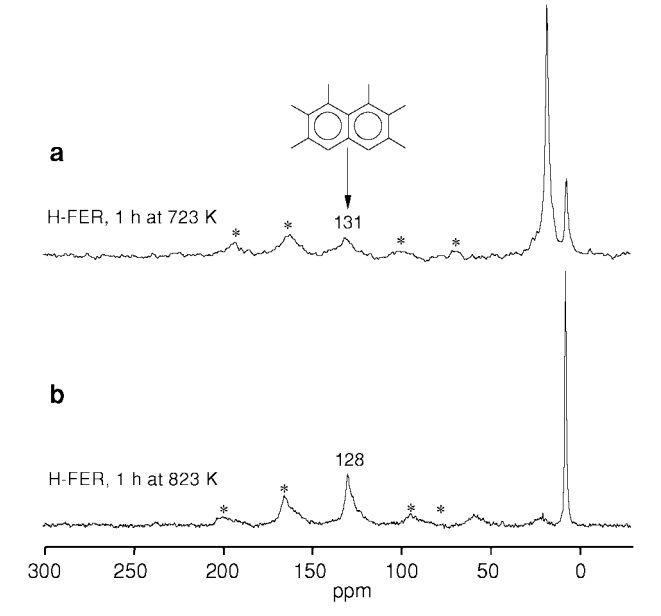


**FIG. 4.** $^{13}C$ CP/MAS NMR spectra of [1-$^{13}C$]-*n*-but-1-ene on H-FER zeolite after reaction at (a) 723 K and (b) 823 K. Asterisks denote spinning sidebands.

## 4. DISCUSSION

This study performs experiments in a closed batch reactor. Reaction conditions are similar to those for the *n*-butene isomerization on a fresh zeolite in a flow reactor. The expected reactions for *n*-butene conversion are as follows: a double-bond-shift reaction to form *n*-but-2-enes, isomerization to isobutene, disproportionation to produce propene and pentenes, hydrogen transfer, and coke formation. It was concluded from previous studies (3, 6–8, 11) that the bimolecular mechanism via dimerization-cracking to isobutene and its disproportionation products prevails on a fresh zeolite sample.

The $^{13}C$ MAS NMR observation of *n*-butene transformation in the batch reactor in the temperature range of 300–823 K allows us to distinguish the following steps of the olefin conversion under static conditions: a double-bond-shift reaction and $^{13}C$-label scrambling, oligomerization (dimerization), conjunct polymerization, formation of polycyclic (condensed) aromatics, formation of a simple aromatic with methane, and ethane evolution.

### *4.1. Double-Bond-Shift Reaction and $^{13}$C-Label Scrambling (300–373 K)*

The formation of *trans*- and *cis*-*n*-but-2-enes from *n*-but-1-ene is observed at 300 K (Fig. 1). This process is fast compared to the process of the selective $^{13}$C-label scrambling. The signals from butenes **2** appear in the spectrum immediately after *n*-butene **1** adsorption on zeolite (Fig. 1, spectrum b), whereas the signal at 126 ppm due to the label scrambling appears in the spectrum only after keeping the sample at 300 K for some days. The appearance of the signal at 126 ppm from the =CH– group of *n*-but-2-enes indicates that the selective $^{13}$C label penetrates from the terminal $CH_3$ group of *n*-but-2-enes **2** into the neighbor inner =CH– group of the linear hydrocarbon skeleton of these isomeric olefins **2** (Fig. 1, spectrum c). This scrambling could be reasonably rationalized in terms of the formation of protonated cyclopropane intermediates on the zeolite (35, 36) as demonstrated in Scheme 1.

The cyclopropane intermediates can be reopened and yield either primary or secondary cations. The former provides the route for the formation of isobutene, and the latter should result in *n*-but-2-enes. The signal at 126 ppm indicates that the protonated cyclopropane is indeed formed as intermediate or transition state, and it is further transformed into butenes **2** with the label at the =CH– group.

Isobutene is not obtained under these conditions. The characteristic narrow signal from methyl groups of isobutene at 24 ppm could not be found and the broad signals from carbons at olefinic double bonds at 111 and 142 ppm were not detected. The signal at 24 ppm occurs if isobutene is adsorbed on the sodium ferrierite (Fig. 6, spectrum a). However, for isobutene adsorbed on H-FER this signal is missing at room temperature. Instead, the signals from the methyl groups of isobutene dimers are observed in the spectrum at 33 ppm (Fig. 6, spectrum b), cf. 2,2-dimethyl-3-hexene, 3,4,4-trimethyl-2-pentene, and

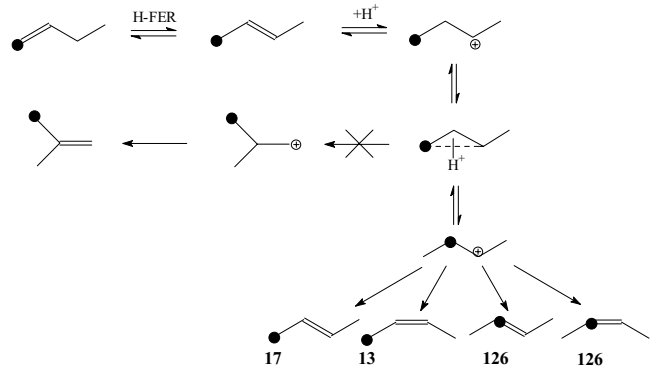


**SCHEME 1.** Double-bond-shift reaction and the $^{13}$C-label scrambling in [1-$^{13}$C]- *n*-but-1-ene on H-FER zeolite at 300–373 K. The black dots denote the $^{13}$C-labeled carbon atoms with chemical shifts indicated nearby.

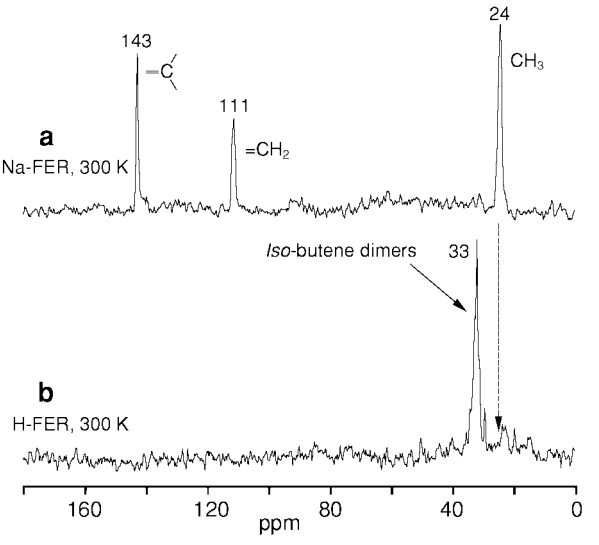


**FIG. 6.** $^{13}$C MAS NMR spectra of ferrierites at 300 K, which are loaded with isobutene: (a) sodium ferrierite (Na-FER), (b) hydrogen ferrierite (H-FER).

2,4,4-trimethyl-1-pentene (17). From this fact we conclude that isobutene reacts during a longer contact time to acid sites, whereas it does not react during the shorter contact time in a flow reactor. It transforms inevitably into a mixture of isobutene dimers under the static conditions of a batch reactor.

It could be assumed that the broad signals at 25 and 33 ppm at temperatures of 300 and 373 K (Fig. 1, spectrum c and d) are due to isobutene dimers, which result from the monomolecular isomerization of *n*-butene via intermediate formation of isobutene and its subsequent dimerization. But Fig. 6 (spectrum b) shows that isobutene dimers exhibit an intense signal at 33 ppm. Thus isobutene is not formed from *n*-butene even as an intermediate. The butene dimers (oligomers) were formed directly from the *n*-butenes **2** in our batch reactor.

From the absence of the signals from isobutene or its dimers under conditions of the $^{13}$C-label scrambling in *n*-but-2-enes (Fig. 1) we conclude that the cyclopropane ring opening (for a monomolecular isomerization pathway) does not occur under these conditions. This is in good agreement with the concept (18, 19) which explains a very low rate of formation of isobutene through a monomolecular mechanism by the necessity of the formation of a highly energetic (compared to the secondary cation) primary cation, which is a precursor of isobutene. Alternatively, the isomerization of a dimeric cation via successive stages of hydrogen and methyl shift reactions toward $C_8^+$ carbenium ion with *tert*-butyl fragment allows avoidance of the intermediacy of the primary cation. Thus, our data support the assumption that a monomolecular isomerization does not take place on a fresh zeolite.

### *4.2. Oligomerization and Conjunct Polymerization (300–523 K)*

The signals from the *n*-butene oligomers (13, 25, and 33 ppm) at temperatures of 300 and 373 K show further that the dimerization of butenes **2** is the more facile process than monomolecular isomerization toward isobutene. The observation of oligomerization (dimerization) supports the possibility of a bimolecular mechanism (Scheme 2), since the formation of isobutene by the bimolecular mechanism requires a dimerization step.

*n*-Butenes **2** convert completely into butene oligomers at 473 K. But neither the signal of isobutene nor the signals due to its dimers appear in the spectra (compare Figs. 2, spectrum a and 3, spectrum a). Philippou *et al.* (17) claimed the formation of isobutene from butene oligomers at this temperature. The increase of the intensity of the signal at 24 ppm with the temperature was assigned to the appearance of isobutene as a reaction product (17). But we have demonstrated in Fig. 6 that isobutene does not exist in its monomeric form on H-FER at room temperature, which is the temperature of spectra registration in the experiments by Philippou *et al.* (17). Therefore, the growth of the signal at 24 ppm should rather be attributed to the increase of the amount of butene oligomers after treatment at 473 K. Alternatively, this signal can be assigned to isobutane, which exhibits a signal with similar chemical shift. It has been reported in numerous $^{13}$C MAS NMR studies (23–25, 37) that isobutane represents a prevailing species in the pattern of alkanes formed from the cracking of oligomers on acidic zeolites at 473–573 K in a batch reactor.

It is well known that *n*-butene converts to isobutene in a flow reactor (3, 11). The different behavior between $^{13}$C MAS NMR studies in the batch reactor and catalytic studies in the flow reactor cannot be explained by a different loading under flow condition. A mixture of 5% *n*-butene-1 in an inert gas of the stream gives a similar loading as used in our batch reactor (one molecule per one acidic site). Therefore, our rationalization of the absence of the signals from isobutene is based on the difference between flow and batch reactor (without continuous feed of the reagent and inert gas carrier). Isobutene, which is possibly formed in the batch reactor, then reoligomerizes again, whereas in a flow reactor it desorbs and cannot reoligomerize in the gas phase.

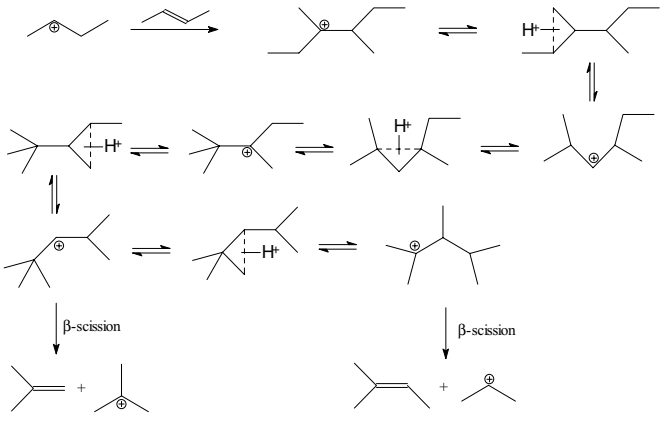


**SCHEME 2.** Oligomerization (dimerization) and cracking processes to provide the pathway for the formation of isobutene via a bimolecular mechanism on H-FER.

One could expect that the increase of the reaction temperature would lead to the cracking of butene oligomers (dimers), producing olefins (isobutene, propene, pentenes) as reaction products and carbenium ions (*tert*-butyl and isopropyl cations) by the $\beta$-scission mechanism (see Scheme 2). However, the main reaction products at 523 K are alkanes and methyl-substituted CPCs with the corresponding signals at 152 and 252 ppm (33) in Fig. 2 (spectrum b). Simultaneous formation of CPCs and alkanes indicates "conjunct polymerization." This process was described for the first time by Ipatieff and Pines (38, 39) for the conversion of isobutene in sulfuric acid. The CPC was identified as a characteristic species formed in conjunct polymerization for the first time by Deno *et al.* (40). CPC on zeolites HY (22) and HZSM-5 (41) and on sulfated zirconia (29) were found to be the species deactivating the catalysts at 473 K in olefin (22, 41), alkane (29), and alcohol conversion (25). Conjunct polymerization can be explained as a multistep process shown in Schemes 2 and 3. It includes the steps of oligomer (dimer) cracking affording carbenium ions like the *tert*-butyl or isopropyl cations (Scheme 2), hydrogen-transfer reactions by hydride abstraction of the formed cations yielding alkanes and hydrogen-deficient charged conjugated double-bond oligomers, which are further converted to the form of the most stable CPC (40) (see Scheme 3). The charged conjugated double-bond oligomers have been already identified by Paze *et al.* (13) in the reaction of *n*-butene conversion on H-FER by UV–vis spectroscopy. But the attribution of the observed bands to the $\pi^* \leftarrow \pi$ transitions at 20000–15000 cm$^{-1}$ (13) to CPCs could not be made unambiguously.

Benzylic cations formed from alkyl aromatics were proposed as the active sites for the *n*-butene isomerization via a pseudo-monomolecular mechanism (9–11). However, CPCs are the only cationic species that are identified for *n*-butene conversion on H-FER and, therefore, they could be considered as the possible active sites for isomerization by pseudo-monomolecular mechanism. CPCs are formed below 623 K (22, 25, 28, 29), which is the usual temperature for an isomerization reaction under flow conditions. But it cannot be excluded that these cations also exist at higher temperature, if the reaction is performed under the flow conditions with a shorter contact time than under the batch condition. Therefore, these cations should not be discarded as the active sites for pseudo-monomolecular *n*-but-1-ene isomerization in the technical processes.

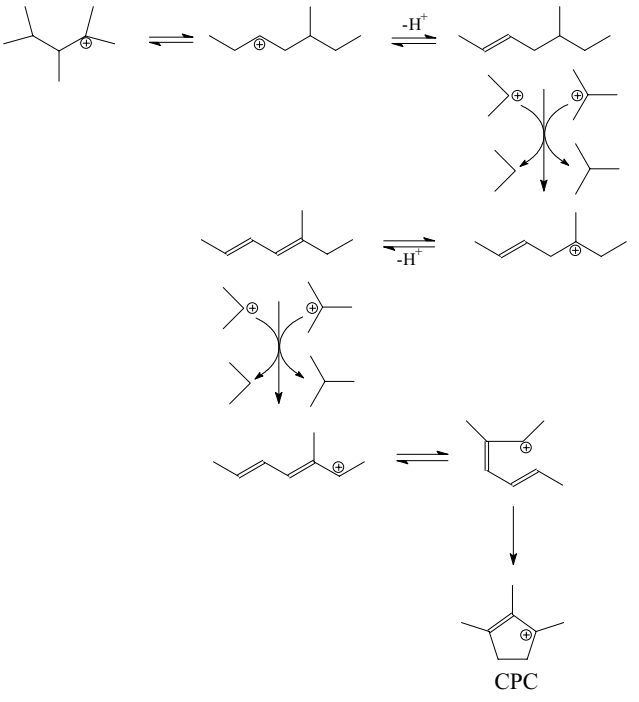


**SCHEME 3.** Conjunct polymerization on H-FER at 473–523 K.

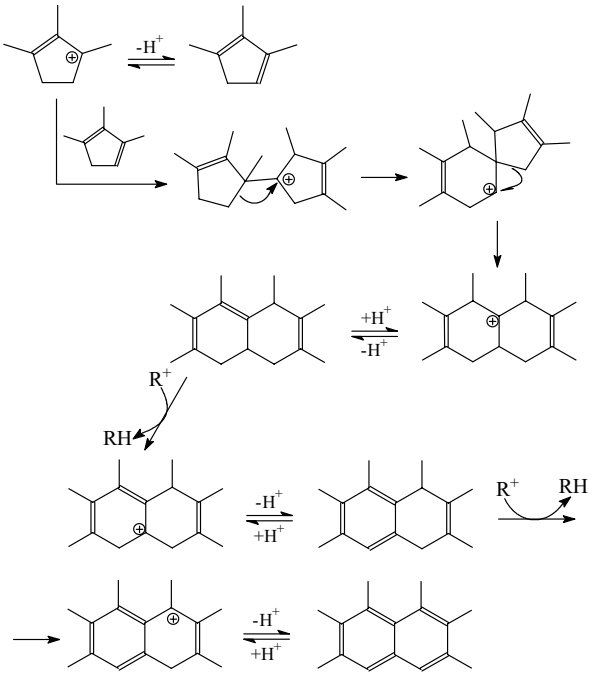


**SCHEME 4.** Formation of condensed aromatics from the CPCs.

### *4.3. Formation of Polycyclic Aromatics (523–723 K)*

Condensed aromatics are already formed at 523 K. Corresponding signals are observed at 130 and 144 ppm in addition to the signals from the CPCs. Further increase of the reaction temperature causes the complete disappearance of the signals from the CPCs. Only condensed aromatics and alkanes were formed at 623 K. CPCs appear at 523 K and disappear at higher temperature. This intermediate appearance allows us to conclude that the CPCs seem to be the precursors of condensed aromatics (coke). The latter presumably forms from the CPCs as shown in Scheme 4. It implies that the formation of the condensed aromatics involves the CPC deprotonation and protonation, its dimerization, $\beta$-scission, and hydrogen transfer by an abstraction of hydrides by the carbenium ions. It should be emphasized that our data do not show the formation of condensed aromatics from a simple one as was proposed earlier for this reaction (11). On the contrary, simple aromatics form from the condensed one as evidenced from the experiments at 823 K.

### *4.4. Formation of Simple Aromatics with Methane and Ethane Evolution (823 K)*

At 823 K condensed aromatics convert to methyl-substituted simple aromatics with an intense and broad signal centered at 128 ppm. It seems to be due to an essential contribution from benzene, which is also formed under this condition (Fig. 4, spectrum b). Simultaneously, the signals from only the light alkanes, methane, and ethane are observed in the spectrum (Fig. 5, spectrum b). In principle, methane and ethane may be formed by the cracking of larger alkanes. The conversion of the condensed aromatics into simple aromatics implies protonation, $\beta$-scission, cycle reopening, and alkyl shift reaction. Methyl and ethyl abstraction can occur and yield methane and

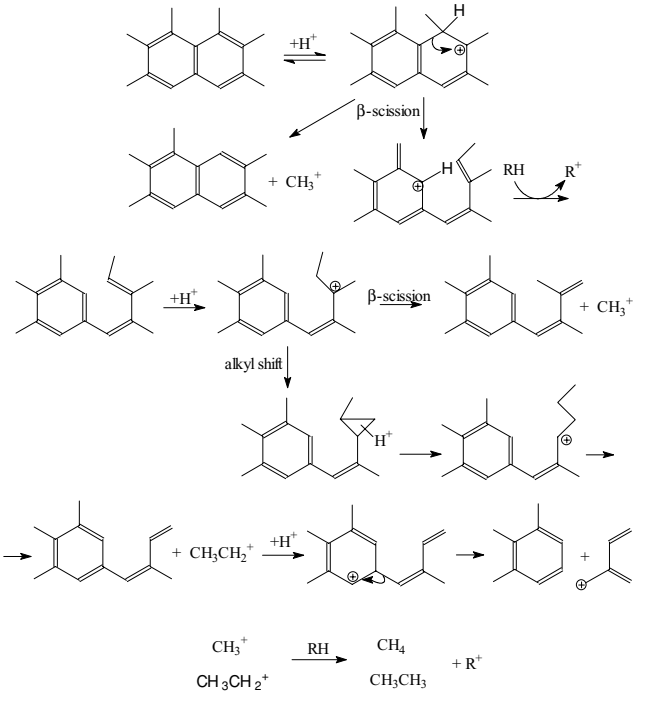


**SCHEME 5.** Formation of simple from condensed aromatics with methane and ethane evolution.

ethane. This pathway for methane and ethane formation from condensed aromatics may be essential at this temperature. The transformation into simple aromatics and $C_1$–$C_2$ alkanes can proceed in accordance with Scheme 5.

## 5. CONCLUSIONS

$^{13}C$ MAS NMR spectroscopy of the temperature-dependent conversion of *n*-but-1-ene on H-FER in a batch reactor offers information about the mechanism of isomerization and the formation of carbonaceous deposits, which is also important for processes in a flow reactor.

The following successive steps in the olefin conversion at increasing temperature of the reaction were distinguished: a double-bond-shift reaction affording *n*-but-2-enes, scrambling of the selective $^{13}C$ label in *n*-but-2-enes, oligomerization (dimerization), conjunct polymerization, formation of condensed aromatics, and formation of simple aromatics.

Selective $^{13}C$-label scrambling in *n*-but-2-ene and oligomerization, as well as the absence of isobutene among the products of *n*-but-1-ene isomerization, provides evidence for a bimolecular pathway of *n*-but-1-ene isomerization on a fresh zeolite via the stages of *n*-but-1-ene dimerization (oligomerization) and cracking of the dimers. Monomolecular isomerization of *n*-but-1-ene into isobutene does not occur on uncoked zeolite samples.

Alkyl-substituted CPCs are the only cationic species observed on H-FER. They, rather than benzylic cations as suggested by Andy *et al.* (11), can serve as the active sites for pseudo-monomolecular isomerization of *n*-butene on the coked zeolite samples.

Carbonaceous deposits, which represent polycyclic aromatics (coke) and deactivate the catalyst in the isomerization reaction, are formed from the alkyl-substituted CPCs, which are produced in the conjunct polymerization process. At higher temperatures, polycyclic aromatics are transformed into simple aromatics with methane and ethane evolution.

## ACKNOWLEDGMENTS

This work was supported by the Deutsche Forschungsgemeinschaft, SFB 294. We are grateful to Prof. Dr. H. Papp, Prof. Dr. J. Kärger, Dr. A. Philippou, Prof. Dr. M. W. Anderson and to the referees for advice.

## REFERENCES

1. Vaughan, P. A., *Acta Crystallogr.* **21**, 983 (1966).
2. Butler, A. C., and Nicolaides, C. P., *Catal. Today* **18**, 443 (1993).
3. Mooiweer, H. H., de Jong, K. P., Kraushaar-Czarnezki, B., Stork, W. H. J., and Krutzen, B. C. H., *Stud. Surf. Sci. Catal.* **84**, 2327 (1994).
4. O'Yong, C.-L., Pellet, R. J., Casey, D. G., Ugolini, J. R., and Sawicki, R. A., *J. Catal.* **151**, 467 (1995).
5. Guisnet, M., Andy, P., Gnep, N. S., Travers, C., and Benazzi, E., *J. Chem. Soc., Chem. Commun.* 1685 (1995).
6. Meriaudeau, P., Bacaud, R., Hung, L. N., and Vu, T. A., *J. Mol. Catal. A* **110**, L177 (1996).
7. Guisnet, M., Andy, P., Gnep, N. S., Benazzi, E., and Travers, C., *J. Catal.* **158**, 551 (1996).
8. Meriaudeau, P., Naccache, C., Le, H. N., Vu, T. A., and Szabo, G., *J. Mol. Catal. A* **123**, L1 (1997).
9. Guisnet, M., Andy, P., Gnep, N. S., Travers, C., and Benazzi, E., *Stud. Surf. Sci. Catal.* **105**, 1365 (1997).
10. Guisnet, M., Andy, P., Boucheffa, Y., Gnep, N. S., Travers, C., and Benazzi, E., *Catal. Lett.* **50**, 159 (1998).
11. Andy, P., Gnep, N. S., Guisnet, M., Benazzi, E., and Travers, C., *J. Catal.* **173**, 322 (1998).
12. Cejka, J., Wichterlova, B., and Sarv, P., *Appl. Catal., A: Gen.* **179**, 217 (1999).
13. Paze, C., Sazak, B., Zecchina, A., and Dwyer, J., *J. Phys. Chem. B* **103**, 9978 (1999).
14. Rutenbeck, D., Papp, H., Ernst, H., and Schwieger, W., *Appl. Catal., A: Gen.* **208**, 153 (2001).
15. Seo, G., Kim, M.-Y., and Kim, J. H., *Catal. Lett.* **67**, 207 (2000).
16. Ivanov, P., and Papp, H., *Langmuir* **16**, 7769 (2000).
17. Philippou, A., Dwyer, J., Ghanbari-Siahkali, A., Paze, C., and Anderson, M. W., *J. Mol. Catal. A* **174**, 223 (2001).
18. Lossing, F. P., and Semeluk, G. P., *Can. J. Chem.* **48**, 955 (1970).
19. Brouwer, D., and Oelderik, J., *Recl. Trav. Chim. Pays-Bas* **87**, 721 (1968).
20. Kondo, J. N., Yoda, E., Hara, M., Wakabayashi, F., and Domen, K., *Stud. Surf. Sci. Catal.* **130C**, 2933 (2000).
21. Petkovic, L. M., and Larsen, G., *J. Catal.* **191**, 1 (2000).
22. Haw, J. F., Richardson, B. R., Oshio, I. S., Lazo, N. D., and Speed, J. A., *J. Am. Chem. Soc.* **111**, 2052 (1989).
23. Anderson, M. W., Sulikowski, B., Barrie, P. J., and Klinowski, J., *J. Phys. Chem.* **94**, 2730 (1990).
24. White, J. L., Lazo, N. D., Richardson, B. R., and Haw, J. F., *J. Catal.* **125**, 260 (1990).
25. Stepanov, A. G., Sidelnikov, V. N., and Zamaraev, K. I., *Chem. Eur. J.* **2**, 157 (1996).
26. Ivanova, I. I., and Corma, A., *J. Phys. Chem. B* **101**, 547 (1997).
27. Stepanov, A. G., Luzgin, M. V., Romannikov, V. N., Sidelnikov, V. N., and Paukshtis, E. A., *J. Catal.* **178**, 466 (1998).
28. Stepanov, A. G., *Russ. Chem. Rev.* **68**, 563 (1999).
29. Luzgin, M. V., Stepanov, A. G., Shmachkova, V. P., and Kotsarenko, N. S., *J. Catal.* **203**, 273 (2001).
30. Hunger, M., and Weitkamp, J., *Angew. Chem., Int. Ed. Engl.* **40**, 2954 (2001).
31. Derouane, E. G., Gilson, J.-P., and Nagy, J. B., *Zeolites* **2**, 42 (1982).
32. van den Berg, J. P., Wolthuizen, J. P., Clague, A. D. H., Hays, G. R., Huis, R., and van Hooff, J. H. C., *J. Catal.* **80**, 130 (1983).
33. Olah, G. A., and Liang, G., *J. Am. Chem. Soc.* **94**, 6434 (1972).
34. Breitmaier, E., and Voelter, W., "13C NMR Spectroscopy, Methods and Applications in Organic Chemistry." VCH, Weinheim, 1978.
35. Brouwer, D. M., and Hogeveen, H., *Prog. Phys. Org. Chem.* **9**, 179 (1972).
36. Saunders, M., Vogel, P., Hagen, E. L., and Rosenfeld, J., *Acc. Chem. Res.* **6**, 53 (1973).
37. Anderson, M. W., and Klinowski, J., *Chem. Phys. Lett.* **172**, 275 (1990).
38. Ipatieff, V. N., and Pines, H., *J. Org. Chem.* **1**, 464 (1936).
39. Pines, H., "The Chemistry of Catalytic Hydrocarbon Conversion." Academic Press, New York, 1981.
40. Deno, N. C., Boyd, D. B., Hodge, J. D., Pittman, J. C. U., and Turner, J. O., *J. Am. Chem. Soc.* **86**, 1745 (1964).
41. Oliver, F. G., Munson, E. J., and Haw, J. F., *J. Phys. Chem.* **96**, 8106 (1992).